

Article

Detecting Connectivity and Spread Pathways of Land Use/Cover Change in a Transboundary Basin Based on the Circuit Theory

Blessing Kavhu ^{1,2,3,*} , Zama Eric Mashimbye ¹  and Linda Luvuno ²

¹ Department of Geography and Environmental Studies, Stellenbosch University, Private Bag X1, Stellenbosch 7602, South Africa

² Centre for Sustainability Transitions, Stellenbosch University, Stellenbosch 7600, South Africa

³ Scientific Services Unit, Zimbabwe Parks and Wildlife Management Authority, Headquarters, Causeway, Harare P.O. Box CY 140, Zimbabwe

* Correspondence: 24580538@sun.ac.za

Abstract: Understanding the spatial spread pathways and connectivity of Land Use/Cover (LULC) change within basins is critical to natural resources management. However, existing studies approach LULC change as distinct patches but ignore the connectivity between them. It is crucial to investigate approaches that can detect the spread pathways of LULC change to aid natural resource management and decision-making. This study aims to evaluate the utility of the Circuit Theory to detect the spread and connectivity of LULC change within the Okavango basin. Patches of LULC change sites that were derived from change detection of LULC based on the Deep Neural Network (DNN) for the period between 2004 and 2020 were used. The changed sites were categorized based on the nature of the change of the classes, namely Category A (natural classes to artificial classes), Category B (artificial classes to natural classes), and Category C (natural classes to natural classes). In order to generate the resistance layer; an ensemble of machine learning algorithms was first calibrated with social-ecological drivers of LULC change and centroids of LULC change patches to determine the susceptibility of the landscape to LULC change. An inverse function was then applied to the susceptibility layer to derive the resistance layer. In order to analyze the connectivity and potential spread pathways of LULC change, the Circuit Theory (CT) model was built for each LULC change category. The CT model was calibrated using the resistance layer and patches of LULC change in Circuitscape 4.0. The corridor validation index was used to evaluate the performance of CT modeling. The use of the CT model calibrated with a resistance layer (derived from susceptibility modeling) successfully established the spread pathways and connectivity of LULC change for all the categories (validation index > 0.60). Novel maps of LULC change spread pathways in the Okavango basin were generated. The spread pathways were found to be concentrated in the northwestern, central, and southern parts of the basin for Category A transitions. As for category B transitions, the spread pathways were mainly concentrated in the northeastern and southern parts of the basin and along the major rivers. While for Category C transitions were found to be spreading from the central towards the southern parts, mainly in areas associated with semi-arid climatic conditions. A total of 186 pinch points (Category A: 57, Category B: 71, Category C: 58) were detected. The pinch points can guide targeted management LULC change through the setting up of conservation areas, forest restoration projects, drought monitoring, and invasive species control programs. This study provides a new decision-making method for targeted LULC change management in transboundary basins. The findings of this study provide insights into underlying processes driving the spread of LULC change and enhanced indicators for the evaluation of LULC spread in complex environments. Such information is crucial to inform land use planning, monitoring, and sustainable natural resource management, particularly water resources.

Keywords: Circuit Theory; connectivity; remote sensing; land cover change; susceptibility modelling; water resources; pinch point; Okavango basin



Citation: Kavhu, B.; Mashimbye, Z.E.; Luvuno, L. Detecting Connectivity and Spread Pathways of Land Use/Cover Change in a Transboundary Basin Based on the Circuit Theory. *Geomatics* **2022**, *2*, 518–539. <https://doi.org/10.3390/geomatics2040028>

Academic Editor: Bruce D. Chapman

Received: 7 October 2022

Accepted: 10 November 2022

Published: 16 November 2022

Publisher's Note: MDPI stays neutral with regard to jurisdictional claims in published maps and institutional affiliations.



Copyright: © 2022 by the authors. Licensee MDPI, Basel, Switzerland. This article is an open access article distributed under the terms and conditions of the Creative Commons Attribution (CC BY) license (<https://creativecommons.org/licenses/by/4.0/>).

1. Introduction

Anthropogenic-driven land use and land cover (LULC) change has been central to natural systems alterations in many environments globally [1–3]. According to Seybold et al. [3] and Martin et al. [4], LULC changes affect climate processes, biogeochemical cycles, nutrient loads, and water resources. Tracking the spatial, temporal, and likely pathways of LULC changes is crucial for landscape management and ecosystem services assessments [5–7]. Owing to their complexity and role as key livelihood support systems for over 60% of the world's population, interest in how LULC changes within transboundary basins (TDBs) and its effect on natural resources distribution is of high priority [8–12]. Most commonly, water resources availability, quality, and distribution within TDBs constitute one of the major contentions among neighboring nations [13–15]. The use of remote sensing and geospatial techniques is entrenched in the detection of LULC change and drivers and for modeling future changes. Hitherto, remote sensing techniques mainly treat LULC change as distinct land patches. Considering LULC as isolated patches pose limitations to understanding the likely pathways of spread for different land cover types. Connectivity-based LULC change analysis frameworks will be beneficial for strategic land management at national, regional, and TDB levels.

Although the spatial-temporal shift in LULC change is well reported, the mechanisms underlying the spread pathways of LULC change across many landscapes remain poorly understood. However, previous studies indicate that LULC is a self-organizing and path-dependent phenomenon [16–19]. Owing to that, understanding the spatial spread pathways followed by LULC change could assist in explaining the arrangement of LULC change occurrences. One of the major advantages of spatial pathways is that they provide essential information about the underlying mechanisms that determine the spread processes [13]. For instance, reduced intensity of spread in a locality could indicate a hindering effect, whereas the increased intensity of spread close to each other could suggest facilitative effects. The use of geostatistical analyses that can quantify spread pathways could help understand underlying processes that influence LULC patterns [14]. This would be an important step toward revealing the underlying mechanisms that promote the spread of LULC change in complex environments and identification of likely spread pinch points, which are crucial for strategic management of LULC change expansion in large environments such as TDBs.

Landscape connectivity is the degree to which the landscape facilitates or impedes movement [15]. The expediency of connectivity has gained prominence in many ecological and biological studies [16,17]. Unlike traditional techniques that predict phenomena as distinct patches and probability of occurrence (susceptibility) maps, connectivity analysis links the distinct patches and inverted probability of occurrence maps (resistance maps) to predict potential spread pathways. In most cases, resistance maps are derived from spatial data layers of factors that impede or facilitate the spread of phenomena. The spread pathways can indicate areas where spread pathways narrow (pinch points), which are crucial for the targeted management of LULC change. For example, detected pinch points for the spread of anthropogenic-related classes could guide the setting up of conservation projects such as protected areas (game reserves and sanctuaries) and put in place measures to reduce urban sprawl [18]. The robustness of connectivity analysis techniques has been proven to be instrumental in the development of more strategic solutions to challenges [19,20]. Despite its tremendous potential to provide spatially explicit predictions on spread pathways that are relevant to sustainable conservation, the application of connectivity analysis in LULC studies remains scanty. Previous studies have been able to predict the distribution and extent of LULC change in TDBs using spatially explicit models that stochastically forecast locations of LULC change patches based on either potential-transition maps that indicate the likelihood of a LULC transition or potential-occurrence maps that indicate the spatial susceptibility of land-cover types [21–25]. Their outputs were mainly patch-based projections of LULC change and the probability of LULC change maps. However, one of their major limitations is that they did not show the interconnectedness of changed land patches in space. In addition, those that were able to model the susceptibility of

LULC failed to use the susceptibility layer in deriving the resistance layer that is required when calibrating connectivity models of LULC change. The use of robust susceptibility modelling techniques such as ensemble models to generate resistance layers could generate more accurate linkages and spread pathways for LULC change in complex environments. Accurate modelling of LULC change spread pathways will allow streamlining of resources on both where change has occurred and the pathways the changes are likely to follow in the long run [26]. Thus, the adoption of such techniques would be crucial to the development of strategic land use plans.

The Circuit Theory (CT) is a recent connectivity modeling technique that has been introduced to predict the dispersal or movement routes of the phenomenon based on concepts and metrics from electrical Circuit Theory. Based on the CT, phenomena are equated to electrons, the landscape as a grid of resistances, and the movement of phenomena across a landscape as the current flowing through a circuit board [27,28]. According to Thayn et al. [29], whereas modeling techniques such as the Least-Cost Path Analysis (LCP) are premised on resistance to model connectivity, the CT presents a more advanced approach to modeling connectivity. LCP is limited as it allows for a single spread path to be detected and does not account for modification by spread features to adopt other potential routes [30]. The strength of the CT is that it allows the detection of multiple pathways. While LCP has been applied to animal movement and fire spread, for example, it may not be applicable to LULC spread modeling owing to its single-path approach against LULC change which is a multidirectional phenomenon. The CT has enabled the modeling of reality much better in many areas of dispersal paths of organisms [31], fire behavior [32], water flow [33], and ecosystem services [26]. For example, Peeler and Smithwick [34] established invasion pathways and spread patterns for Cheatgrass (*Bromus tectorum*) in the Greater Yellowstone using CT modeling. Howey [35] evaluated the past mobility to a regionally significant ceremonial earthwork in the Northern Great Lakes during the Late Prehistory using CT modeling. Wieringa et al. [36] applied CT modeling to successfully predict the migration routes of migratory bats. Thayn [29] identified the most accurate path, which was followed by Hernando de Soto as he crossed the Appalachian Mountains (between Tennessee and North Carolina) using CT modelling. These studies managed to successfully establish the spread pathways for organisms, fire and water. Similar to the aforementioned phenomena, the CT maybe useful for modelling the spread mechanisms of LULC change across a landscape [37]. Also, similar to modelling the spread of previously studied phenomena (organisms, fires and water), aspects that facilitate or impede the spread of LULC can benefit from modeling using CT to detect the potential spread pathways of LULC across the landscape. We believe that such dynamic modelling will go a long way to reveal future patterns of landscape change thus enhancing management and decision making.

Despite the increased appreciation of CT modeling's potential to establish the spread of phenomena across landscapes, to the best of the knowledge of the authors, no studies have explored the utility of the CT theory in LULC changes studies. This is an important gap that needs to be filled to generate spatially explicit information on the spread of LULC change as a preamble to the development of strategic land-use plans. The CT requires a resistance layer which is commonly derived from suitability layers in many ecological studies [38–40]. This study exploits a LULC susceptibility (synonym to suitability) layer generated based on an ensemble of machine learning (ML) in our previous study [41] to compute a resistance layer for use in CT. Understanding the connectivity pathways of LULC change would aid in the development of targeted measures to address the distribution and allocation of resources, for example, water resources.

Using the Okavango basin as a test site, this study borrows ideas from ecological, biological, and electrical research and uses CT modeling to assess the connectivity and spread of LULC change. In order to aid the accomplishment of the aim of this investigation, the following specific objectives were delineated: (1) to assess the value of LULC change susceptibility in modeling spread and connectivity of LULC change, and (2) to model the

spread pathways and pinch points of LULC based on CT. The results of the study are envisaged to contribute to knowledge on geospatial landscape change modeling and are interpreted in the context of advocating best practices for landscape management. This would aid decision-making to enhance resource conservation, and optimization of resource allocation to mitigate conflict, particularly for TDBs where access and use of resources are contentious.

Study Area

This study was conducted in a transboundary basin, the Okavango basin, in southern Africa (see Figure 1). The basin is situated on a longitude range between 16° E and 24° E and a latitude range between 12° S and 21° S. The basin is shared between three countries, namely Botswana, Angola, and Namibia. The Okavango basin has the fourth longest river system in Southern Africa, which starts in Angola with its two main tributaries (Cuito and Cubango rivers) and ends in Botswana at the renowned Okavango Delta [42]. The river system is one of the key livelihood sources for communities living in the Okavango basin [43].

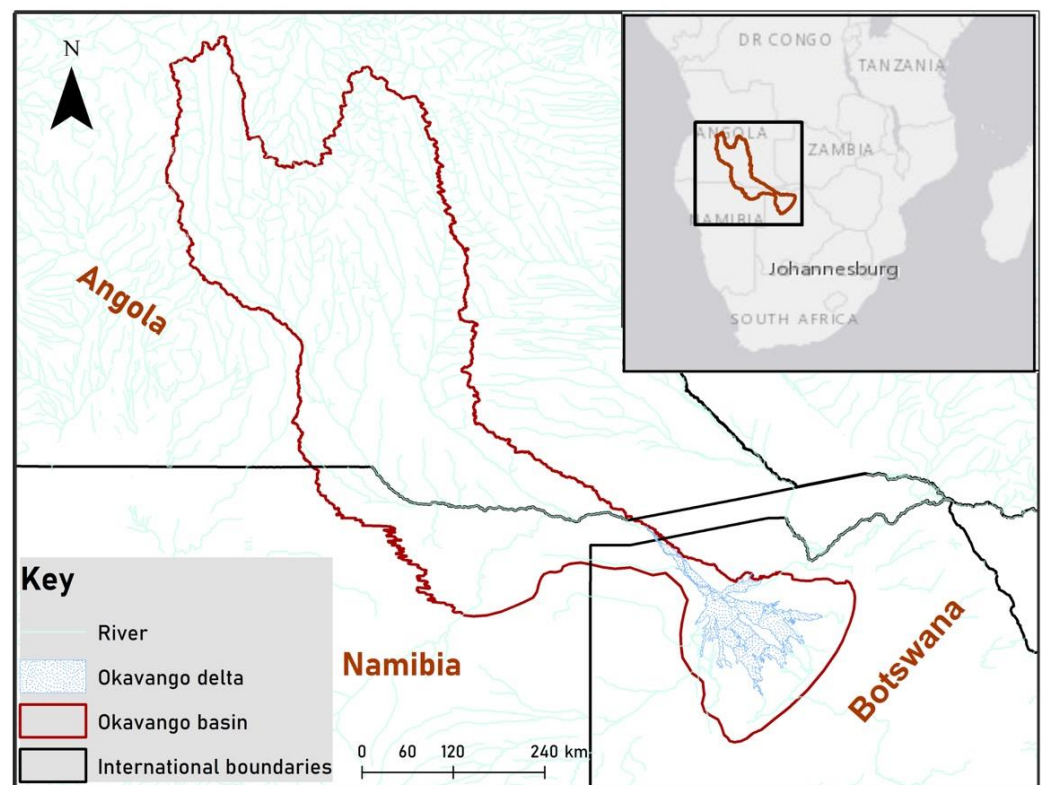


Figure 1. Study area map showing the location of the Okavango basin.

The climate of the Okavango basin is semi-arid and seasonal, marked by an annual mean temperature of 20 °C [44]. High temperatures are commonly experienced during the dry summer season, which poses thermal stress to some flora and fauna. The basin receives unimodal summer rainfall rains that are received between November and April and are commonly associated with mid-season dry spells [45]. Some dry days can extend for a long period resulting in droughts.

Modeling connectivity using the CT theory requires data to be encoded as resistance. LULC data for 2004, 2013, and 2020 and social-ecological drivers of LULC change were used to generate resistance layers. The preprocessing and analysis of data based on CT are explained below.

2. Methods

The study was designed to assess the value of the CT in assessing the spread and connectivity of LULC change and evaluate the distribution pattern of the LULC change site in the Okavango basin. CT modeling was run on Circuitscape 4.0. The workflow of the study design is depicted in Figure 2.

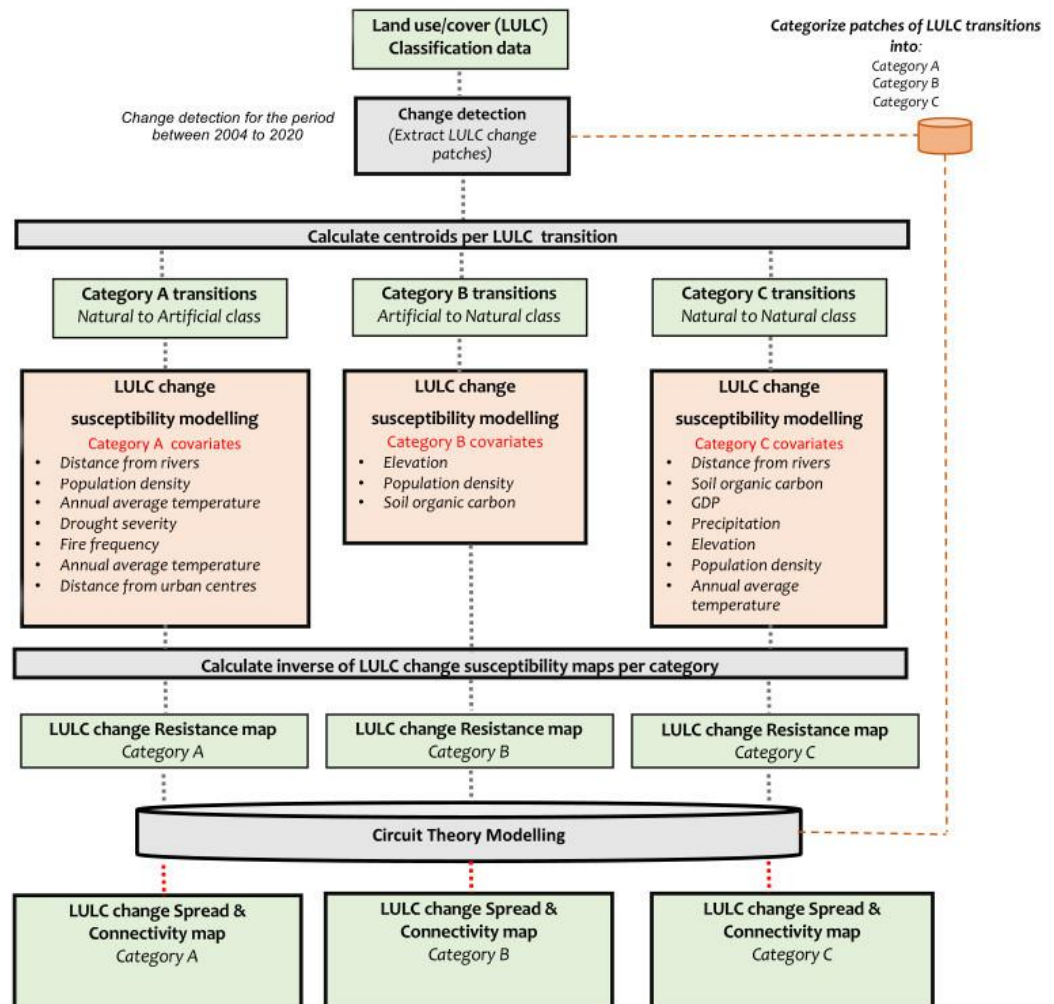


Figure 2. Study methodology workflow. The LULC classification data are derived from results by Kavhu et al. [46]. Covariates for each category were derived from results by Kavhu et al. [41].

This study builds from our previous work [41,46]. In Kavhu et al. [46], we found that post-feature selected and climate-based regionalization improved the accuracy of LULC classification for both Machine Learning and Deep learning techniques within the Okavango, a transboundary basin. The most accurate LULC product was based on the Deep neural network (DNN) classification. For Kavhu et al. [41], the utility of machine learning techniques and ensemble modeling to explain the social-ecological drivers of LULC within the Okavango basin was investigated. Social-ecological drivers of LULC were characterized. The most accurate LULC product and the social-ecological drivers generated in previous studies are used in this study. For more detailed descriptions of methods for LULC classification, change detection, and the characterization of social-ecological drivers, readers should refer to Kavhu et al. [46] and Kavhu et al. [41].

2.1. LULC Classification and Change Detection

In order to determine the LULC classifications, Landsat 5 and Landsat 8 OLI images captured during June for the years 2004, 2013, and 2020 in the Okavango basin were

used. The images were supplemented with spectral features, which comprised Orthogonal and Ratio-based spectral indices. Sample points for eight LULC classes, namely bare land, built-up land, bushland, forest/woodland, grassland, cultivated land, water, and wetland to train the spectral datasets were sourced from the Okavango River Basin Water Commission (OKACOM) geodatabase and National Geographic Okavango and Wilderness Project (NGOWP). Additional samples were generated from digitizing high-resolution satellite imagery from Google Earth. Climate-based regionalization of the study site and feature selection based on the Random Forest-based Recursive feature elimination were implemented to enhance LULC change accuracy. The Deep neural network (DNN) was used for LULC classification in R statistics (See Supplementary Figure S1 for LULC change results). Details of how the DNN was parameterized and the study site was segmented are found in Kavhu et al. [46].

The post-classification change analysis was performed through an overlay analysis of two-time steps ((2004–2013) and (2013–2020)) to detect changed sites [1]. Based on the overlay analysis transition matrix for the intersection of each pair of land cover maps was generated. Centroids of LULC transitions were determined and categorized into three based on the initial class and final class: Category A—transitions (from natural classes to artificial classes); Category B—transitions (from artificial classes to natural classes); and Category C—transitions (from natural classes to another natural class). In this study, the cultivated class was considered to be an artificial class. The rationale for the categorization of LULC transitions is to present transitions in a way that is manageable to practitioners. LULC Categories, transitions, and the number of centroid points for each transition are summarized in Table 1.

Table 1. Shows a summary of categories of LULC transitions based on initial class and final class where Category A have transitions from natural classes to artificial classes, Category B have transitions from artificial classes to natural classes, and Category C have transitions from natural classes to another natural class—adopted from Kavhu et al. [41].

Category	Transition ID	Transition	Number of Centroid Points
A	A1	Water to Cultivated	299
	A2	Woodland to built-up	508
	A3	Woodland to cultivated	23,972
	A4	Grassland to built-up	142
	A5	Grassland to cultivated	7720
	A6	Shrubland to cultivated	453
	A7	Wetland to cultivated	56
B	B1	Cultivated to built-up	1909
	B2	Cultivated to woodland	236
	B3	Cultivated to grassland	4816
	B4	Cultivated to shrubland	463
C	C1	Water to woodland	438
	C2	Water to grassland	70
	C3	Woodland to grassland	66,658
	C4	Woodland to shrubland	12,784
	C5	Grassland to water	1042
	C6	Grassland to shrubland	34,238
	C7	Grassland to wetland	21
	C8	Shrubland to woodland	10,037
	C9	Shrubland to grassland	34,654
	C10	Shrubland to wetland	18
	C11	Wetland to woodland	72
	C12	Wetland to grassland	56
	C13	Wetland to shrubland	46

2.2. Modelling Susceptibility of LULC Change

To model the susceptibility of LULC change in the Okavango basin, we used an ensemble of machine learning models based on centroids of change transitions and already

established social-ecological drivers of LULC change in the Okavango basin. Ensemble models for the three LULC change categories were separately built from a set of singular machine learning models that include Random Forest (RF), Classification Tree Analysis (CTA), Maximum Entropy (MaxENT), Gradient Boosting Model (GBM), and the Artificial Neural Network (ANN). Ensembles of machine learning were considered as they were found to have high predictive accuracy and are capable of effectively deducing patterns from big data [47]. In this study, the ensemble model was built in R statistics using the BIOMOD2 package [48]. The final LULC susceptibility map shows values that range from 0 to 1, where areas with a susceptibility of 0 are not susceptible to LULC change, and those with 1 are highly susceptible. Full details of how the model was parameterized were described in Kavhu et al. [41]. Below are LULC change susceptibility maps for the Okavango basin per category (See Figure 3).

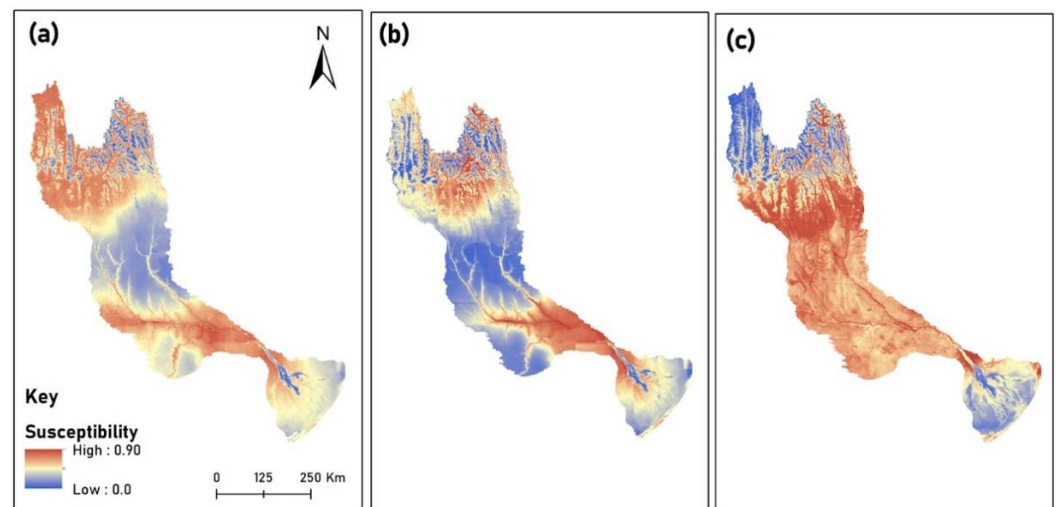


Figure 3. The map shows the LULC change susceptibility maps for different LULC change transitions were; (a) transition from natural to artificial, (b) transition from artificial to natural, (c) transition from natural-to-natural classes.

2.3. Mapping LULC Change Resistance Surface—An Input to Circuit Theory Modelling

The CT model requires a landscape resistance surface layer that describes the cost of moving phenomena through each grid cell as input [17]. In this study, the LULC change susceptibility layer was considered to be synonymous with LULC change permeability. Hence, the inverse function was applied to the LULC change susceptibility layer to derive LULC change resistance following recommendations by McRae et al. [15]. In other words, areas that are highly susceptible to LULC change were considered to present low resistance values and vice versa. This linear transformation is based on the notion that factors that facilitate movement have a direct inverse relationship with those that are resistant to movement [49,50]. Below are the LULC change resistance layers for the three categories of transitions that were used to encode resistance layers for CT modeling in this study (see Figure 4).

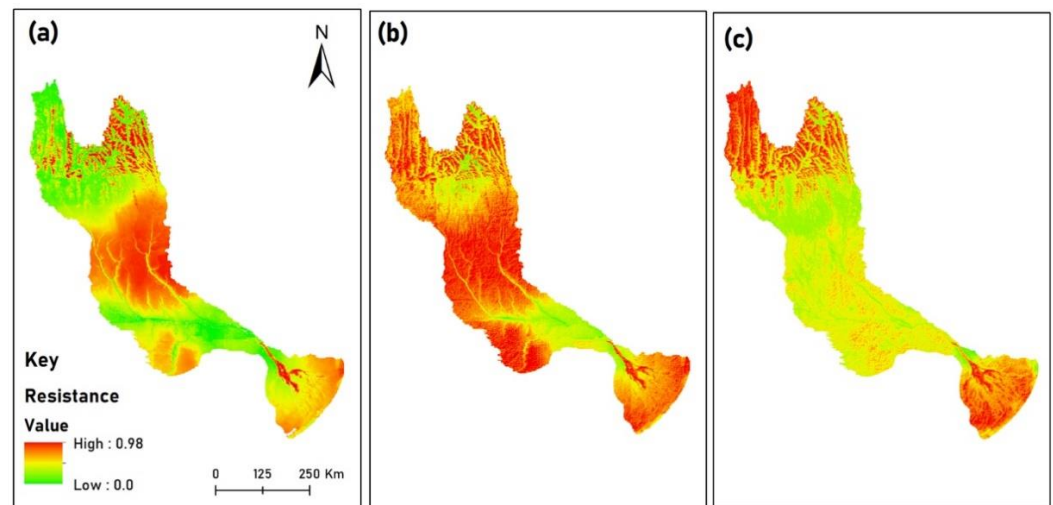


Figure 4. The map shows the LULC change resistance maps for different LULC change transitions were; (a) transition from natural to artificial, (b) transition from artificial to natural, (c) transition from natural-to-natural classes.

2.4. Connectivity Modelling Based on the Circuit Theory

Connectivity between LULC change patches was modeled using CT modeling based on Circuitscape 4.0 [15,27]. CT modeling equates the concept of the flow of charge through a circuit board to the spread of LULC change in a landscape. It applies Ohms law which states that when voltage is applied to a resistor, the amount of current that passes through the resistor depends on applied voltage and resistance. In simple terms, the lower the resistance, the greater the conductance (current). As is the case with an electrical circuit, the CT model treats a circuit as a network consisting of nodes and resistors. It also applies the basic concepts of resistance, conductance, current, and voltage. Table 2 provides the definitions of the electrical terminologies and their related explanation in LULC change studies [51].

Table 2. LULC change spread explanation of electrical terminology.

Electrical Terminology	LULC Change Studies Explanation When Using CT Modelling
Resistance—the opposition that resistors offer to the flow of electrical current	The opposition that landscape offers to the spread of LULC change
Conductance—inverse of resistance, which describes the resistance’s ability to pass current	Synonymous with LULC change permeability
Current—the rate of flow of electric charge past a node or resistance	The rate of LULC change past a landscape
Voltage—the difference in electric potential between two nodes	The probability of LULC change leaving one location spreading to a certain location before another location

In Circuitscape, the CT model runs on the resistance layer, using the Markovian random walk functionality to calculate the total resistance and its opposite current between pairs of LULC change patches at different locations. The areas of least resistance across the landscape are the most probable areas for LULC spread. The CT model produces a resultant map with multiple paths of cumulative current that shows the potential intensity of LULC change flow at each pixel. Grid cells with high current values represent the spread pathways for LULC change, while those with lower values show areas with low potential for LULC change spread [34].

In order to model the connectivity of LULC change in Circuitscape, two input data layers are required, namely the surface resistance layer and locations of LULC change sites. In this study, patches of LULC change served as locations of LULC change sites, and the LULC change surface resistance layer described in Section 2.3 served as the resistance input. Prior to modeling, LULC change patches that belong to the same category were merged using Qgis 2.4 (www.qgis.org, accessed on 12 July 2020) (See Supplementary Figure S2 for the distribution of patches of LULC change). Patches of LULC changes for each category were randomly split, of which 80% were used for training and 20% for validation. Centroids of validation patches were determined to generate validation points in Qgis 2.4. Circuitscape produces a cumulative current layer which shows the connectivity flow of phenomena in a landscape. In order to enhance visualization of cumulative current values together with other features, contours of cumulative current values were extracted from grid layers in Arcmap.

To map the pinch points for LULC change spread, we used the circuit theory-based Linkage Mapper 2.0.0 (<https://linkagemapper.org>, accessed on 7 March 2022). The pinch point helps to identify locations of spread that are crucial to the spread of a LULC in the basin. Such locations are useful for researchers and land managers to develop targeted measures to manage LULC change.

2.5. Validation of Connectivity Models

In order to validate the connectivity outputs, the corridor score validation index was used following Lalechère and Bergès [52]. The index is based on the hypothesis that locations of validation patches concentrate close to predicted connectivity corridors. In this study, the connectivity corridors were generated from thresholding of the cumulative current output. A quantile threshold approach was used at different levels, namely the 55th, 65th, and 75th quantiles, following Lalechère and Bergès [52]. The quantile with the highest validation index was adopted and vectorized for further analysis. The formula below was used to derive the validation index.

$$\text{Validation index} = \frac{1}{N} \sum_{n=1}^N \left(\frac{D_{\text{random}i} - D_{\text{observed}}}{D_{\text{random}i}} \right) \quad (1)$$

where N is the number of random validations draw i , $D_{\text{random}i}$ is the average euclidean distance to corridors from randomly selected points in the landscape for draw i , and D_{observed} is the average euclidean distance to the predicted corridors from the validation points. A validation index value of close to 1 indicates that the validation points are close to the corridor in terms of resistance distance, and the corridor concentrates the predicted connectivity flows. While a validation index of 0 denotes that the corridor does not concentrate on the predicted connectivity flows. A negative index means that the matrix, not the connectivity corridor, concentrates the potential dispersal flows [52].

3. Results

Figures 5–10 show the results for cumulative current maps for transition categories A, B, and C. High cumulative current values (current range between 0.74 to 4.5) are observed mainly in the north, central, and southern parts of the Okavango basin for Category A transitions (Refer to Figures 5 and 6). These areas cover parts of Angola, Namibia, and Botswana. In the northern part, high cumulative values seem to be mainly spreading towards the west and north-western directions connecting areas between Menongue and Chitembo at a latitude range between 12° S and 15° S (Figures 5A and 6). In the south, an interesting pattern is observed where high cumulative current values (ranging between 0.74 to 3.33) spread from the central parts towards the southern parts of the basin connecting areas between Rundu and Maun at a longitude range of 18° E to 24° E via the edges of the Okavango delta (Refer to Figures 5B,C and 6). A total of 57 pinch points were detected in this category, and their distribution seems to follow the distribution patterns of high cumulative current values (See Figure 5A1–C1). It can be seen that high cumulative current

values are radiating from towns and rivers on which current values abruptly increase in their environs (from current of 0.37 to 3.33) (See Figure 6). This indicates how anthropogenic classes will likely spread at the expense of natural vegetation in the Okavango basin. On the other hand, low cumulative current values (less than 0.37) are observed in this category on the north-eastern parts, a large portion of the central part, and portions of the south-central and south-eastern parts (see Figures 5A and 6). The spread pathways of Category A seem to be fairly connected throughout the basin (Figure 5). The validation index of connectivity in this category is 0.72, which indicates that the connectivity model is accurate.

In general, it appears that Category A transitions will most likely spread in the northwestern and north-eastern parts of the northern part of the basin. This transition will also spread from the mid-southern part of the basin to the southeastern parts. The pinch points are fairly spread out along major spread pathways. The spread pathways and distribution patterns of pinch points of this category seem to be mainly aligned with proximity to towns and rivers.

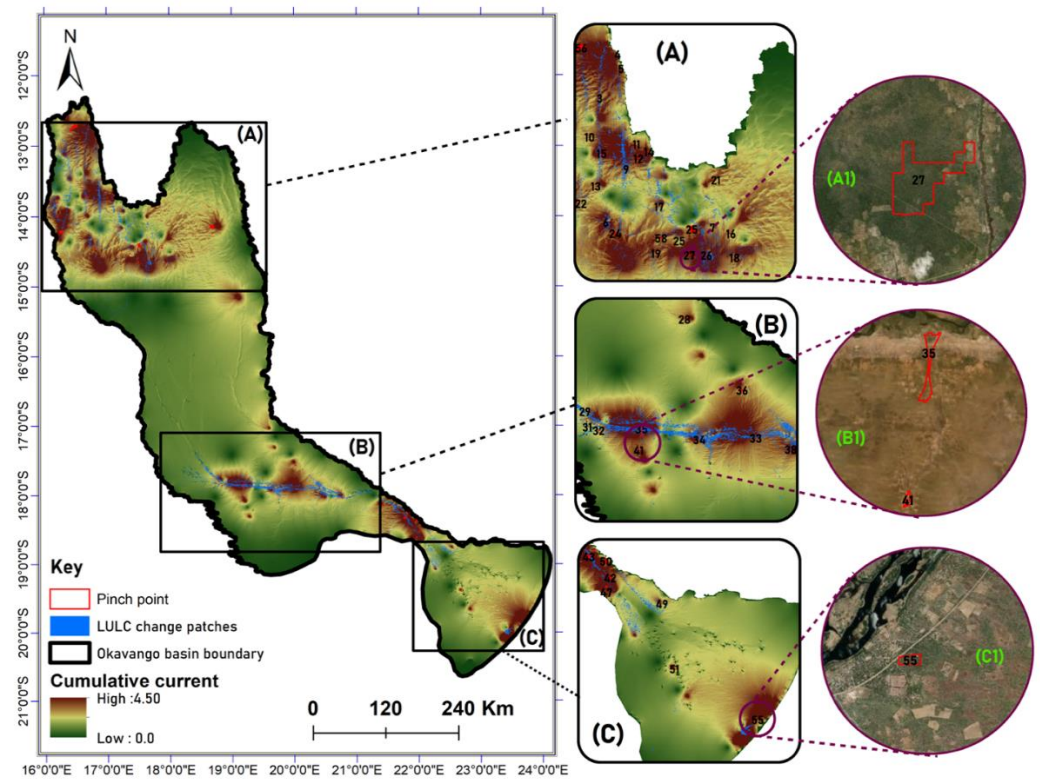


Figure 5. The map shows the cumulative current map and pinch points for Category A transitions (from natural to artificial classes). The subfigures (A–C) highlight areas of the basin with high cumulative current density and subfigures (A1–C1) indicate locations of selected pinch points overlaid on satellite images to show how pinch points appear on the ground.

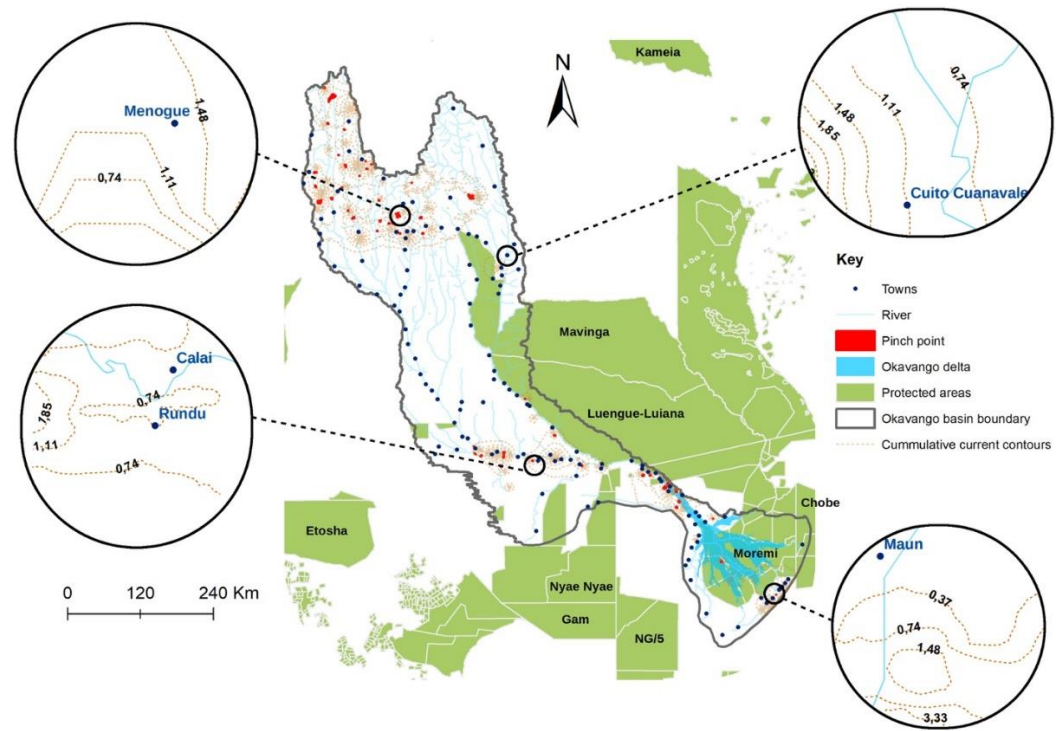


Figure 6. The map shows contours of cumulative current for Category A transitions (from natural to artificial classes) in relation to towns and rivers, and protected areas. The subfigures highlight how current ranges are influenced by the locations of selected towns in the basin.

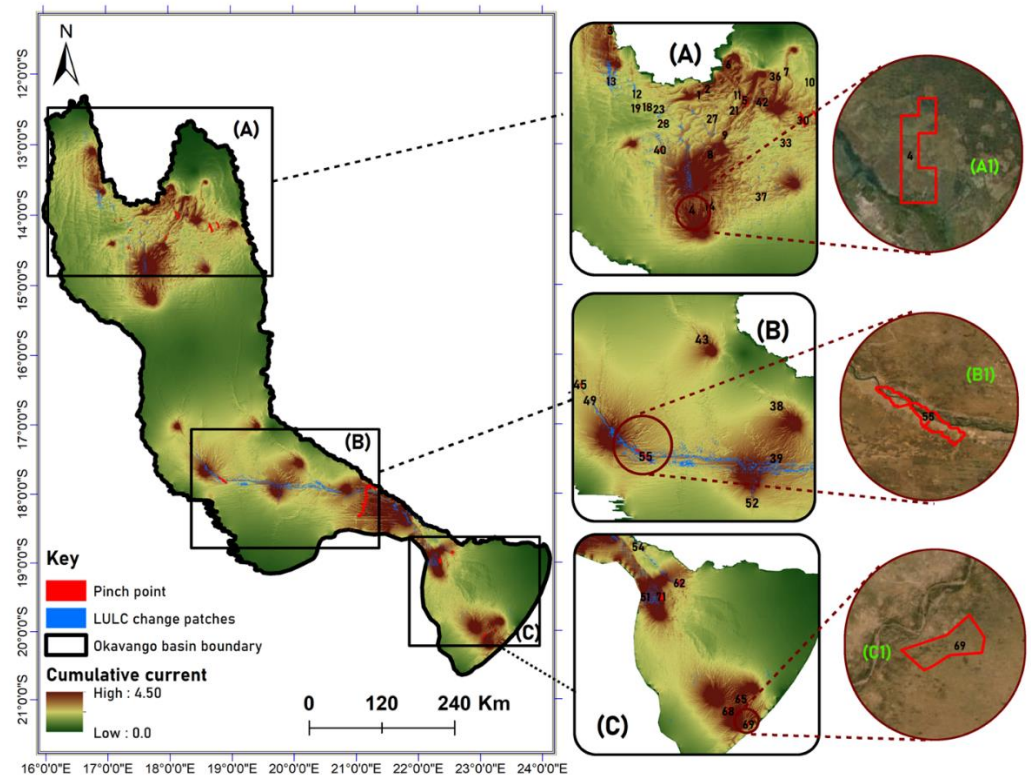


Figure 7. The map shows the cumulative current map and pinch points for Category B transitions (from artificial to natural classes). The subfigures (A–C) highlight areas of the basin with high cumulative current density and subfigures (A1–C1) indicate locations of selected pinch points overlaid on satellite images to show how pinch points appear on the ground.

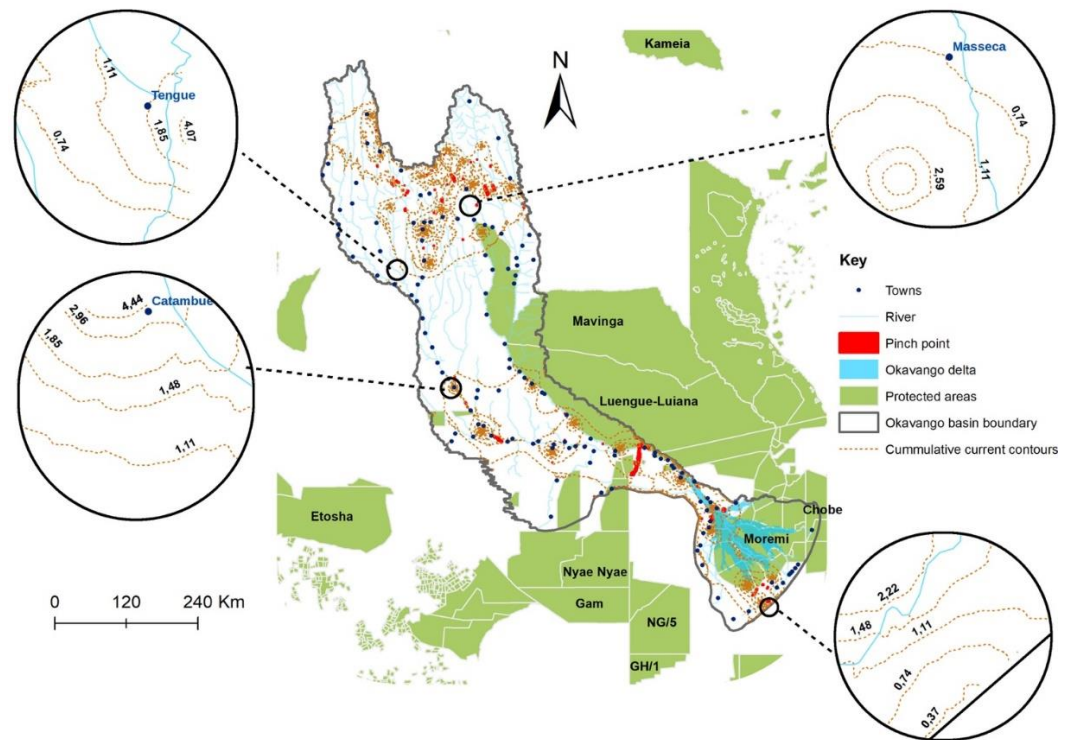


Figure 8. The map shows the contours of cumulative current for Category B transitions (from artificial to natural classes) in relation to towns and rivers, and protected areas. The subfigures highlight how current ranges are influenced by the locations of selected towns and rivers in the basin.

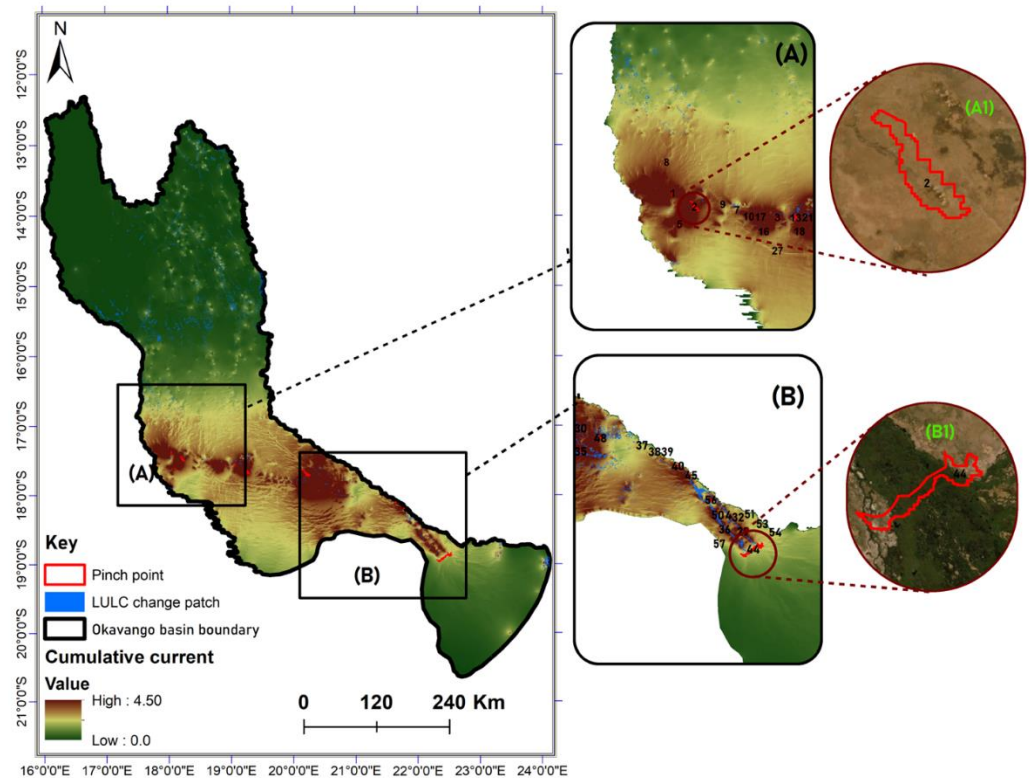


Figure 9. The map shows the cumulative current map and pinch points for Category C transitions (from natural-to-natural classes). The subfigures (A,B) highlight areas of the basin with high cumulative current density and subfigures (A1,B1) indicate locations of selected pinch points overlaid on satellite images to show how pinch points appear on the ground.

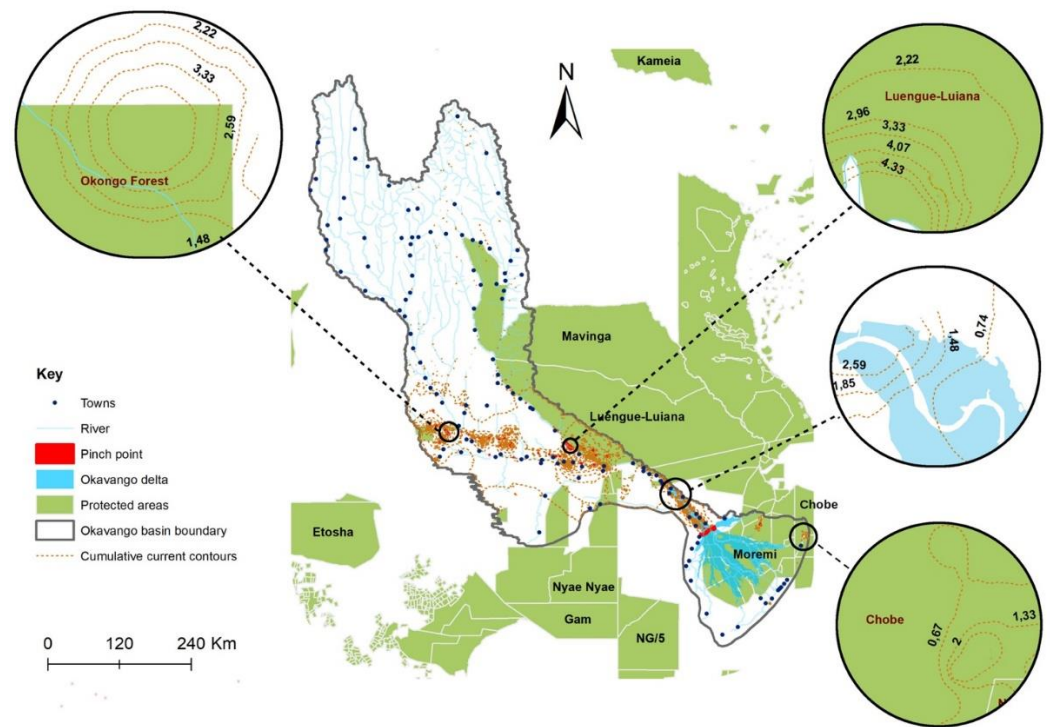


Figure 10. The map shows contours of cumulative current for Category C transitions (from natural-to-natural classes) in relation to towns and rivers and protected areas. The subfigures highlight how current ranges are influenced by the locations of selected towns and rivers in the basin.

With regards to Category B transitions, high cumulative current values are mainly found in the north and southern parts of the basin (current range from 0.74 to 4.44), covering parts of Angola and Botswana (Refer to Figures 7 and 8). In the north, high cumulative values (current range 0.74 to 4.07) seem to be spreading in the northeastern direction connecting areas between Menongue and Cuito Cuanavale between a longitude range of 17° E to 19° E (Refer to Figure 7A). In the south, another pattern is observed where high current values appear to be spreading following the western edges of the Okavango Delta panhandle towards the southern parts (Refer to Figures 7C and 8). A total of 71 pinch points were detected in this category. Such as the spread pathways, locations of pinch points are mainly concentrated in the north and southern parts of the basin. It can be seen that the spread pathways seem to align with the locations of towns and rivers both in the northern and southern parts (Refer to Figure 7). The spread patterns for Category B show how natural vegetation will recuperate from cultivated land. Low cumulative current values (less than 0.74) were observed in the central parts of the basin, mainly in parts of Namibia between a latitude range of 15° S to 17° S. Areas of low cumulative values seem to be aligned to the limited availability of river channels. As seen by a large area with a low cumulative current in the middle portion of the basin, the spread pathways in the northern part appear to be completely disconnected from the ones in the southern part of the basin (Figure 6). The spread of Category B transition in the southern part is highly connected (see Figure 8). A validation index of 0.68 for Category B transitions is observed, which shows that the model is fairly accurate.

Overall, Category B transitions reveal two centers of spread pathways, one situated in the northern side of the basin while the other is within the mid-southern and south-eastern sections of the basin. The two areas of spread are completely disconnected. It appears that Category B transitions on the northern part will spread in the northwestern and north-eastern directions. The distribution of pinch points is in tandem with that of spread pathways. Category B spread in the mid-southern and south-eastern portions of the basin are highly linked. There are some areas in the mid-southern and south-eastern parts where

Category B seems restricted from expanding, as evidenced by low cumulative current values (Figure 7) and the absence of cumulative contours (Figure 8). These areas seem to be associated with low river density when compared to the north and southern parts of the basin.

As can be seen in Figures 9 and 10, Category C transitions spread is restricted to the mid-southern part of the Okavango basin. This spread will most likely move towards the southeastern portion of the basin and only be restricted by the delta (Figure 10). It seems that there is little chance for Category C to spread to the northern part of the basin. The spread of LULC change of this category seems to cover mainly parts of Botswana and Namibia. It can be seen that the high cumulative values in this category dominate in areas with low anthropogenic activities and are associated with protected areas (see Figure 10). Areas with low cumulative current values indicate how natural vegetation will change from one class to another as a result of natural processes such as droughts, floods, and invasion. A total of 58 pinch points were observed in this category, and these can be used for targeted management of the natural processes that drive LULC change. Low cumulative current values (less than 0.67) are recorded in the due north and southern areas of the Okavango basin, covering major parts of Angola and Botswana, respectively. Low cumulative values areas appear to be associated with permanently established towns and wetlands (Okavango delta) (Figure 10). The validation index for this category is 0.66, which indicates that the connectivity model is accurate.

4. Discussion

Using susceptibility maps of LULC change, this study revealed that CT modeling could successfully detect the spread and connectivity between LULC change patches. This is so because it consistently established the spread and connectivity of three different categories of LULC change transitions. These transitions are Category A (transition from natural to artificial); Category B (from artificial to natural); and Category C (from natural-to-natural classes). In addition, observations at selected validation sites confirmed the occurrence of change along predicted connectivity areas, as evidenced by validation index values higher than 0.5. Moreover, the predicted spread patterns in this study pass through locations of LULC change identified in previous work that predicted the distribution of LULC in the basin [41]. While previous studies were successful in predicting future LULC change, their results were based on discrete patches of LULC change which promotes a piecemeal approach to LULC change management. Other studies have successfully used spatially explicit models based on different sets of environmental factors to predict the probability of occurrence (susceptibility) of LULC change [24,25,53]. However, one of the shortcomings of these studies is that they could not deduce the spread pathways of LULC change and strategic pinch points for intervention. The novelty of this study rests in that it combines LULC change patches and susceptibility maps to establish the spread pathways and connectivity of LULC change patches. The advantage of connectivity analysis is that it provides explicit spatial information on the links (multi-paths) that exist between distinct change patches and provides predictions of potential spread direction and pathways based on factors that impede or facilitate the spread of LULC change. It also helps to identify points where spread pathways narrow (pinch-points), and such points are crucial for targeted intervention when monitoring LULC change. This information would be beneficial for developing strategic measures to address challenges associated with the change in LULC, both on where change has occurred and the likely pathways changes it would follow in the future, particularly in situations where LULC change is contagious.

The usefulness of CT modeling has already been explored when evaluating the spread and movement pathways of phenomena in ecology, hydrology, and archaeology. For example, Gray and Dickson [32] used CT to model landscape-scale fire connectivity for resource and fire management in the Sonoran Desert in the USA. They used data for large fires, wind speed, and wind direction to compute a conductance layer for use in CT. They established that the spread of the fire was higher in lower elevations and areas

with lower slopes and topographic roughness. Brennan et al. [54] used the CT and GPS data from six species to evaluate connectivity at multiple scales within the Kavango-Zambezi transform frontier conservation landscape in southern Africa. They evaluated the effects of linear barriers, natural habitat types, and anthropogenic land use on animal movement. They modeled landscape resistance using step selection functions to compare habitat characteristics at 'used' and 'available' steps to quantify an animal's selection and avoidance of landscape attributes during movement. They established that there were many intact areas across the landscape with diffuse current flow and that fences, rivers, roads, and areas of anthropogenic land use acted as barriers to animal movement. The current study used a LULC susceptibility layer to compute a resistance (for use in CT) derived from an ensemble of machine learning models based on centroids of change transitions and social-ecological drivers of LULC change in the Okavango basin. No studies that applied the LULC change susceptibility and CT modeling to evaluate LULC change spread were found in the literature.

This investigation yielded important results of likely pathways of spread of different LULC transitions and their pinch points (186) using the CT. The findings of the study show that LULC change spread pathways for Category A were widely connected across the basin with relatively high current values diffusing from existing towns (See Figure 6). This is consistent with previous studies which reported that anthropogenic activities such as the expansion of built-up areas and agricultural areas occur close to urban centers [55–58]. This is so due to the main drivers of these activities being attracted to areas with the most preferred resources, such as access to jobs, development, and market for agricultural produce [59]. The results of this study contest those of Woldeamayyat and Genovese [60], who recorded the isolation of patches of urban expansion in Addis Abba, Ethiopia. This can be attributed to the unplanned allocation of land for the city's key development projects, which resulted in isolated urban patches in Addis Abba, as observed by Terfa et al. [61]. Unlike in Addis Abba, where there are uncontrolled urbanization and development projects, the Okavango basin has controlled anthropogenic developments that are ensured by the Okavango River Basin Commission (OKACOM) [62–65]. Future studies should compare patterns of LULC change distribution in areas with contrasting land management regimes.

The spread of high cumulative current values for Category A transitions was found to be concentrated in the northwestern, central, and southern parts of the basin. These areas are most likely going to experience an increased intensity of the spread of LULC change linked to the expansion of anthropogenic activities such as urban and cultivated areas. Most of the spread pathways in this category were found to be radiating from major urban centers, namely Mentogwe in the north, Chitembo in the northwest, Rundu in the central parts, and Maun in the south. Pinch points for the spread of LULC transitions in this category were located close to established urban centers and existing cultivated fields. Locations of pinch points can be used for setting conservation areas, ecovillages, and urban boundaries [66]. Kgathi et al. [43] assert that access to jobs, development, and markets for agricultural produce drive occupation of land situated close to towns. Hence management strategies to curb this, such as the redevelopment of inner core regions and urban consolidation in towns situated close to pinch points, can be put in place [67,68]. The north-western and north-eastern spread pathways are highly connected and expansive. This will most likely have a significant impact on water consumption for domestic, agriculture, and for industries, leading to less water for the southern parts of the basin. Natural vegetation, including wetlands, will most probably be impacted by this spread due to the possible expansion of fields, which may impact water quality. Predicted spread pathways in this study are in line with the distribution of expansion in anthropogenic activities in the Okavango basin described in previous studies. For instance, Andersson [69] conducted a study that found that expansions will likely occur in and around Rundu, Menongue, and Cuito Canavale. Our study provides spread pathways through other districts that were not previously reported in the literature. This study is unique in that it yielded LULC change connectivity based on exhaustive and recent data. Furthermore, this study covered the

entire Okavango basin using satellite imagery of the period between 2004 and 2020. In contrast, Andersson [69] only covered the northern part of the basin using satellite imagery from 1973 to 2001. For Category A, low cumulative current values were observed in areas situated in the northeastern, central, and southwestern parts of the basin (Figure 5). This is likely due to the presence of landmines in the northeastern districts such as Mexico, which restricts anthropogenic activities [70]. According to Finch et al. [71], there are hunting concessions in areas close to the central parts of the basin and wildlife management areas in the southwestern part of the basin, such as Chobe National Park. This study's findings of low to medium cumulative current values (less than 0.37) in these areas are indicative of barriers to anthropogenic activities due to these protected areas (see Figure 10).

With regards to Category B transitions, we observed connectivity of LULC changes mainly in the northern and the mid-south and south-eastern parts of the basin. The two centers of connectivity seem to be disconnected from each other, as observed by a large area of low cumulative current in the middle portion of the basin. The transitions which are found in this category are that of previously cultivated classes that changed to natural classes. Hence, the observed distribution pattern could be a reflection of the past distribution of cultivated fields that were abandoned in the Okavango basin. Cultivated fields often cluster in areas characterized by viable lands that are suitable for agricultural production and often close to major water sources such as Cuito and Cubango in the basin [72,73]. In the Okavango basin, most rural communities migrated to towns during the post-Angolan war period [43,74]. Rural out-migration often leads to a decrease in rural populations, low demand for agricultural space, and limited workforce hence the abandonment of cultivated fields [75]. Owing to that, the abandoned cultivated lands in the Okavango basin will likely maintain the same connected pattern of formerly cultivated lands. A total of 71 pinch points that were found in this study are potential targets for vegetation restoration projects by ecologists and land managers. Woods and Elliot [76] proposed direct seeding for forest restoration as a strategy to promote ecosystem recovery in abandoned fields. Hence, adopting such techniques at pinch points and other spread pathways that are situated close to rivers would be helpful to enhance ecological integrity of the Okavango basin. Category B spread also appears to move into the pan handle of the delta (see Figure 8). This is most likely due to people shifting from one field to another due to soil degrading over time or moving into areas that were previously under water as water recedes during drier years [77]. This area constantly experiences droughts and flooding [78]. So, some fields will be inaccessible during periods of flooding and vice versa. Setting up of alternative livelihood strategies such as ecotourism and apiculture projects for communities living along spread pathways adjacent to the panhandle and other floodplains could assist in promoting recuperation of former cultivated lands [79,80]. Our findings supplement a growing body work reporting on management of abandonment of cultivated fields.

The connectivity of Category C transitions (natural to natural classes) was found to be restricted to the mid-southern part of the basin. This category displays a very low chance of moving to the northern part of the basin. Moreover, it seems to be restricted to moving into the delta. This could be due to the localized nature of driving factors of this transition that could be perpetuated by existing climatic conditions. Literature is replete with evidence of the conversion of one natural vegetation cover to another as a consequence of localized factors such as fire, invasion, and climate variability in the Okavango basin. For instance, Heintz [81] found that woody species were lost to shrubs and grasses due to frequent fires in the basin. Forno and Smith [82] established that the extent of wetlands in the basin was reduced due to invasion by alien aquatic weeds, such as *Salvinia molesta* (salvinia) and *Eichhornia crassipes* (water hyacinth). Ringrose et al. [83] found that drought conditions have caused island woody vegetation cover invading wetlands to form clusters of dense woodlands. According to Heintz [81], most transitions that involve the loss of wetland areas (for example, C1, C2, C11, C12, C13) are a result of highly frequent fires, which tend to affect certain localities in a landscape. The area that is concentrated by spread pathways for this

transition primarily falls within the Hot semi-arid (Bsh) Koppen climate zone and does not go beyond this zone to the north. The semi-arid regions are renowned to be associated with the aforementioned drivers of this LULC transition (namely droughts, natural fires and invasion) [84–86]. Promoting research on targeted invasive species monitoring and allowing communities to collect thatch grass at pinch points, particularly those situated in protected areas, to reduce fuel load could be helpful in reducing species invasion and wildfires in the basin. Moreover, sustainable water management strategies (for example, introducing a water quota) in the upstream areas would ensure continual supply downstream to reduce the chances of drought conditions which promote spread of Category A transitions [87]. For example, this study found that spread of Category A transitions in the southern part is bound by the Okavango delta which is a demonstration of how lots of water facilitates maintenance of habitats for vegetation species that are endemic to this area [88]. Findings of this study aid insight into the interaction between climate, natural events, water systems and ecological integrity.

As can be observed in Figures 5, 7 and 9, the extent of spread for transitions from natural to anthropogenic classes (Category A) generally looks larger compared to the other transitions (Category B and C). This is in line with other studies that reported the dominance of anthropogenic activities in driving LULC change [89–91]. Anthropogenic activities are often rapid and tend to affect large tracts of land when compared to natural processes [5,92–94]. This study is novel in the sense that it yielded spatially explicit information on the extent of LULC change spread, including detecting likely pathways of the spread for the different categories investigated. We are convinced that this study lays a good foundation for future investigations on LULC change, detecting likely pathways, pinch points, and landscape modeling. Such information is crucial to inform land use planning, monitoring, and decision-making.

Though findings from this study provide important contributions to improving the mapping and monitoring of LULC change in TDBs, it should be noted that there are some limitations associated with this study. The study did not incorporate in the generation of the resistance surface layer other drivers of LULC change, such as landmines that remained during the war in Angola due to data unavailability. This is also the first time that a resistance layer derived from LULC susceptibility modeling has been used in LULC connectivity modeling. This study exploited the success of a previous study where we created a LULC susceptibility layer using social-ecological data based on an ensemble of Machine Learning. Other authors may use different datasets and spatial resolutions for such purposes. Future studies may benefit from including landmine distribution data when generating surface resistance data for connectivity of LULC change in the Okavango basin. This study was conducted at a regional scale which tends to generalize other predictors which could be influencing the connectivity of LULC change at a local scale. Future studies conducted on smaller scales may help reveal local trends that could not be discerned by this investigation as it was conducted at a regional scale.

5. Conclusions

This study aimed to investigate the value of the CT to detect the connectivity and distribution of LULC changes in the Okavango basin. The specific objectives were to:

- (1) assess the role of LULC change susceptibility in modeling spread and connectivity of LULC change, and
- (2) model the spread pathways of LULC based on CT.

The study found that:

- (a) CT and connectivity modeling provides a new decision-making technique for predicting the spread pathways of LULC change.
- (b) there is a connectivity of LULC change observations for all categories of LULC change in the Okavango basin, which is a testament that LULC change has a facilitative effect. Hence, management focus should not only be given to patches of LULC change sites but also to potential spread pathways.

- (c) A total of 186 pinch points (57 for Category A, 71 for Category B, and 58 for Category C) were detected. The pinch points can be used for targeted management LULC change through the setting up of conservation areas, forest restoration projects, drought monitoring, and invasive species control.

We conclude that the application of CT modelling is crucial to targeted management of LULC change in complex and transboundary systems. Unlike traditional methods, CT modeling provides a novel approach to establishing reliable spread pathways and strategic pinch points of LULC change. While the spread of anthropogenic-related change transitions is widespread across the basin, natural change transitions are mainly restricted to semi-arid climatic zones. The predicted spread of anthropogenic-related LULC change in the northern parts of the basin will likely impact the quality and availability of water downstream of the Okavango river.

Supplementary Materials: The following supporting information can be downloaded at: <https://www.mdpi.com/article/10.3390/geomatics2040028/s1>, Figure S1: Land use/cover classification outputs during the years 2004 (a), 2013 (b), and 2020 (c) in the Okavango basin. Figure S2: Map shows the LULC change patches for different LULC change transitions were; (a) transition from natural to artificial, (b) transition from artificial to natural, (c) transition from natural-to-natural classes.

Author Contributions: Conceptualization: B.K., Z.E.M. and L.L.; Methodology: B.K., Z.E.M. and L.L.; Writing—original draft: B.K., Z.E.M. and L.L.; Writing—review and editing: B.K., Z.E.M. and L.L. All authors have read and agreed to the published version of the manuscript.

Funding: The authors received funding from the USAID Resilient Waters Project for this research under prime contract number 72067418C00007.

Institutional Review Board Statement: Not applicable.

Informed Consent Statement: Not applicable.

Data Availability Statement: Training data which was used in this study are available upon request from the authors.

Acknowledgments: We thank USAID Resilient Waters for funding this project, implemented under prime contract number 72067418C00007. Our appreciation goes to the OKACOM and Okavango Wildland Trust for supplying us with some ground data which was used in this study. Many thanks to the anonymous reviewers for their insightful comments that were helpful in improving this manuscript. Blessing is grateful to Amanda October and Cornelia Jacobs for their extensive logistical help during the project.

Conflicts of Interest: The authors declare that there exists no competing financial interest or personal relationships that could appear to influence the work reported in this study.

References

1. Münch, Z.; Gibson, L.; Palmer, A. Monitoring Effects of Land Cover Change on Biophysical Drivers in Rangelands Using Albedo. *Land* **2019**, *8*, 33. [[CrossRef](#)]
2. Digra, M.; Dhir, R.; Sharma, N. Land use land cover classification of remote sensing images based on the deep learning approaches: A statistical analysis and review. *Arab. J. Geosci.* **2022**, *15*, 1003. [[CrossRef](#)]
3. Seybold, E.; Gold, A.J.; Inamdar, S.P.; Adair, C.; Bowden, W.B.; Vaughan, M.C.; Pradhanang, S.M.; Addy, K.; Shanley, J.B.; Vermilyea, A. Influence of land use and hydrologic variability on seasonal dissolved organic carbon and nitrate export: Insights from a multi-year regional analysis for the northeastern USA. *Biogeochemistry* **2019**, *146*, 31–49. [[CrossRef](#)]
4. Martin, S.L.; Hayes, D.B.; Kendall, A.D.; Hyndman, D.W. The land-use legacy effect: Towards a mechanistic understanding of time-lagged water quality responses to land use/cover. *Sci. Total Environ.* **2017**, *579*, 1794–1803. [[CrossRef](#)] [[PubMed](#)]
5. Wang, L.; Jia, Y.; Li, X.; Gong, P. Analysing the Driving Forces and Environmental Effects of Urban Expansion by Mapping the Speed and Acceleration of Built-Up Areas in China between 1978 and 2017. *Remote Sens.* **2020**, *12*, 3929. [[CrossRef](#)]
6. Govender, T.; Dube, T.; Shoko, C. Remote sensing of land use-land cover change and climate variability on hydrological processes in Sub-Saharan Africa: Key scientific strides and challenges. *Geocarto Int.* **2022**, 1–25. [[CrossRef](#)]
7. Mati, B.M.; Morgan, R.P.; Gichuki, F.N.; Quinton, J.N.; Brewer, T.R.; Liniger, H.P. Assessment of erosion hazard with the USLE and GIS: A case study of the Upper Ewaso Ng'iro North basin of Kenya. *Int. J. Appl. Earth Obs. Geoinf.* **2000**, *2*, 78–86. [[CrossRef](#)]

8. Domisch, S.; Kakouei, K.; Martínez-López, J.; Bagstad, K.J.; Magrach, A.; Balbi, S.; Villa, F.; Funk, A.; Hein, T.; Borgwardt, F. Social equity shapes zone-selection: Balancing aquatic biodiversity conservation and ecosystem services delivery in the transboundary Danube River Basin. *Sci. Total Environ.* **2019**, *656*, 797–807. [[CrossRef](#)]
9. Hirbo Gelebo, A.; Kasiviswanathan, K.S.; Khare, D.; Pingale, S.M. Assessment of spatial and temporal distribution of surface water balance in a data-scarce African transboundary river basin. *Hydrol. Sci. J.* **2022**, *67*, 1561–1581. [[CrossRef](#)]
10. Derdour, A.; Benkaddour, Y.; Bendahou, B. Application of remote sensing and GIS to assess groundwater potential in the transboundary watershed of the Chott-El-Gharbi (Algerian–Moroccan border). *Appl. Water Sci.* **2022**, *12*, 136. [[CrossRef](#)]
11. Wu, C.; Du, B.; Cui, X.; Zhang, L. A post-classification change detection method based on iterative slow feature analysis and Bayesian soft fusion. *Remote Sens. Environ.* **2017**, *199*, 241–255. [[CrossRef](#)]
12. Yang, Y.; Nan, Y.; Liu, Z.; Zhang, D.; Sun, Y. Direct and indirect losses of natural habitat caused by future urban expansion in the transnational area of Changbai Mountain. *Sustain. Cities Soc.* **2020**, *63*, 102487. [[CrossRef](#)]
13. Velázquez, E.; Martínez, I.; Getzin, S.; Moloney, K.A.; Wiegand, T. An evaluation of the state of spatial point pattern analysis in ecology. *Ecography* **2016**, *39*, 1042–1055. [[CrossRef](#)]
14. Kamusoko, C.; Kamusoko, O.W.; Chikati, E.; Gamba, J. Mapping Urban and Peri-Urban Land Cover in Zimbabwe: Challenges and Opportunities. *Geomatics* **2021**, *1*, 114–147. [[CrossRef](#)]
15. McRae, B.H.; Dickson, B.G.; Keitt, T.H.; Shah, V.B. Using circuit theory to model connectivity in ecology, evolution, and conservation. *Ecology* **2008**, *89*, 2712–2724. [[CrossRef](#)]
16. Cushman, S.A.; McRae, B.; Adriaensen, F.; Beier, P.; Shirley, M.; Zeller, K. Biological corridors and connectivity. *Key Top. Conserv. Biol.* **2013**, *2*, 384–404.
17. Zeller, K.A.; McGarigal, K.; Whiteley, A.R. Estimating landscape resistance to movement: A review. *Landscape Ecol.* **2012**, *27*, 777–797. [[CrossRef](#)]
18. Cao, G.; Feng, C.; Tao, R. Local “land finance” in China’s urban expansion: Challenges and solutions. *China World Econ.* **2008**, *16*, 19–30. [[CrossRef](#)]
19. Wang, Y.; Qu, Z.; Zhong, Q.; Zhang, Q.; Zhang, L.; Zhang, R.; Yi, Y.; Zhang, G.; Li, X.; Liu, J. Delimitation of ecological corridors in a highly urbanizing region based on circuit theory and MSPA. *Ecol. Indic.* **2022**, *142*, 109258. [[CrossRef](#)]
20. Yu, H.; Gu, X.; Liu, G.; Fan, X.; Zhao, Q.; Zhang, Q. Construction of regional ecological security patterns based on multi-criteria decision making and circuit theory. *Remote Sens.* **2022**, *14*, 527. [[CrossRef](#)]
21. Verburg, P.H.; Soepboer, W.; Veldkamp, A.; Limpitad, R.; Espaldon, V.; Mastura, S.S.A. Modeling the Spatial Dynamics of Regional Land Use: The CLUE-S Model. *Environ. Manag.* **2002**, *30*, 391–405. [[CrossRef](#)]
22. Castella, J.-C.; Pheng Kam, S.; Dinh Quang, D.; Verburg, P.H.; Thai Hoanh, C. Combining top-down and bottom-up modelling approaches of land use/cover change to support public policies: Application to sustainable management of natural resources in northern Vietnam. *Land Use Policy* **2007**, *24*, 531–545. [[CrossRef](#)]
23. Poelmans, L.; Van Rompaey, A. Complexity and performance of urban expansion models. *Comput. Environ. Urban Syst.* **2010**, *34*, 17–27. [[CrossRef](#)]
24. Talukdar, S.; Eibek, K.U.; Akhter, S.; Ziaul, S.K.; Islam, A.R.M.T.; Mallick, J. Modeling fragmentation probability of land-use and land-cover using the bagging, random forest and random subspace in the Teesta River Basin, Bangladesh. *Ecol. Indic.* **2021**, *126*, 107612. [[CrossRef](#)]
25. Jamali, A.A.; Ghorbani Kalkhajeh, R. Urban environmental and land cover change analysis using the scatter plot, kernel, and neural network methods. *Arab. J. Geosci.* **2019**, *12*, 100. [[CrossRef](#)]
26. Dickson, B.G.; Albano, C.M.; Anantharaman, R.; Beier, P.; Fargione, J.; Graves, T.A.; Gray, M.E.; Hall, K.R.; Lawler, J.J.; Leonard, P.B. Circuit-theory applications to connectivity science and conservation. *Conserv. Biol.* **2019**, *33*, 239–249. [[CrossRef](#)]
27. McRae, B.H.; Shah, V.B.; Edelman, A. Circuitscape: Modeling landscape connectivity to promote conservation and human health. *Nat. Conserv.* **2016**, *14*. [[CrossRef](#)]
28. Anantharaman, R.; Hall, K.; Shah, V.; Edelman, A. Circuitscape in Julia: High Performance Connectivity Modelling to Support Conservation Decisions. *arXiv* **2019**. [[CrossRef](#)]
29. Thayn, J.B.; Sampeck, K.; Spaccapaniccia, M. Refining Hernando de Soto’s route using electric circuit theory and Circuitscape. *Prof. Geogr.* **2016**, *68*, 595–602. [[CrossRef](#)]
30. Beyond Least Cost Paths: Circuit Theory, Maritime Mobility and Patterns of Urbanism in the Roman Adriatic-ScienceDirect. Available online: <https://www.sciencedirect.com/science/article/pii/S0305440321002089> (accessed on 6 October 2022).
31. Lohay, G.G.; Riggio, J.; Lobora, A.L.; Kissui, B.M.; Morrison, T.A. Wildlife movements and landscape connectivity in the Tarangire Ecosystem. In *Tarangire: Human-Wildlife Coexistence in a Fragmented Ecosystem*; Springer: Berlin/Heidelberg, Germany, 2022; pp. 255–276.
32. Gray, M.E.; Dickson, B.G. A new model of landscape-scale fire connectivity applied to resource and fire management in the Sonoran Desert, USA. *Ecol. Appl.* **2015**, *25*, 1099–1113. [[CrossRef](#)]
33. Tahavori, M.; Kallesøe, C.S.; Leth, J.; Wisniewski, R. Modeling of water supply systems: Circuit theoretic approach. In Proceedings of the 2012 7th IEEE Conference on Industrial Electronics and Applications (ICIEA), Singapore, 18–20 July 2012; pp. 1561–1566.
34. Peeler, J.L.; Smithwick, E.A. Exploring invasibility with species distribution modeling: How does fire promote cheatgrass (*Bromus tectorum*) invasion within lower montane forests? *Divers. Distrib.* **2018**, *24*, 1308–1320. [[CrossRef](#)]

35. Howey, M.C. Multiple pathways across past landscapes: Circuit theory as a complementary geospatial method to least cost path for modeling past movement. *J. Archaeol. Sci.* **2011**, *38*, 2523–2535. [[CrossRef](#)]
36. Wieringa, J.G.; Carstens, B.C.; Gibbs, H.L. Predicting migration routes for three species of migratory bats using species distribution models. *PeerJ* **2021**, *9*, e11177. [[CrossRef](#)] [[PubMed](#)]
37. Bennie, J.; Hodgson, J.A.; Lawson, C.R.; Holloway, C.T.R.; Roy, D.B.; Brereton, T.; Thomas, C.D.; Wilson, R.J. Range expansion through fragmented landscapes under a variable climate. *Ecol. Lett.* **2013**, *16*, 921–929. [[CrossRef](#)] [[PubMed](#)]
38. Dupas, S.; Le Ru, B.; Branca, A.; Faure, N.; Gigot, G.; Campagne, P.; Sezonlin, M.; Ndemah, R.; Ong'Amo, G.; Calatayud, P.-A. Phylogeography in continuous space: Coupling species distribution models and circuit theory to assess the effect of contiguous migration at different climatic periods on genetic differentiation in *Busseola fusca* (Lepidoptera: Noctuidae). *Mol. Ecol.* **2014**, *23*, 2313–2325. [[CrossRef](#)]
39. Melles, S.J.; Chu, C.; Alofs, K.M.; Jackson, D.A. Potential spread of Great Lakes fishes given climate change and proposed dams: An approach using circuit theory to evaluate invasion risk. *Landsc. Ecol.* **2015**, *30*, 919–935. [[CrossRef](#)]
40. Ahmadi, M.; Nezami Balouchi, B.; Jowkar, H.; Hemami, M.-R.; Fadakar, D.; Malakouti-Khah, S.; Ostrowski, S. Combining landscape suitability and habitat connectivity to conserve the last surviving population of cheetah in Asia. *Divers. Distrib.* **2017**, *23*, 592–603. [[CrossRef](#)]
41. Kavhu, B.; Eric Mashimbye, Z.; Luvuno, L. Characterising social-ecological drivers of landuse/cover change in a complex transboundary basin using singular or ensemble machine learning. *Remote Sens. Appl. Soc. Environ.* **2022**, *27*, 100773. [[CrossRef](#)]
42. Wolski, P.; Savenije, H.H.G.; Murray-Hudson, M.; Gumbricht, T. Modelling of the flooding in the Okavango Delta, Botswana, using a hybrid reservoir-GIS model. *J. Hydrol.* **2006**, *331*, 58–72. [[CrossRef](#)]
43. Kgathi, D.L.; Ngwenya, B.N.; Wilk, J. Shocks and rural livelihoods in the Okavango Delta, Botswana. *Dev. S. Afr.* **2007**, *24*, 289–308. [[CrossRef](#)]
44. Mendelsohn, J.; El Obeid, S. *Okavango River: The Flow of a Lifeline*; Struik: Cape Town, South Africa, 2004.
45. Wilk, J.; Kniveton, D.; Andersson, L.; Layberry, R.; Todd, M.C.; Hughes, D.; Ringrose, S.; Vanderpost, C. Estimating rainfall and water balance over the Okavango River Basin for hydrological applications. *J. Hydrol.* **2006**, *331*, 18–29. [[CrossRef](#)]
46. Kavhu, B.; Mashimbye, Z.E.; Luvuno, L. Climate-based regionalization and inclusion of spectral indices for enhancing transboundary land-use/cover classification using deep learning and machine learning. *Remote Sens.* **2021**, *13*, 5054. [[CrossRef](#)]
47. Dietterich, T.G. Ensemble Methods in Machine Learning. In *Multiple Classifier Systems*; Springer: Berlin/Heidelberg, Germany, 2000; pp. 1–15.
48. Thuiller, W.; Georges, D.; Engler, R.; Breiner, F. biomod2: Ensemble platform for species distribution modeling. *R Package Version* **2013**, *2*, r560.
49. Ghoddousi, A.; Bleyhl, B.; Sichau, C.; Ashayeri, D.; Moghadas, P.; Sepahvand, P.; Kh Hamidi, A.; Soofi, M.; Kuemmerle, T. Mapping connectivity and conflict risk to identify safe corridors for the Persian leopard. *Landsc. Ecol.* **2020**, *35*, 1809–1825. [[CrossRef](#)]
50. Mateo-Sánchez, M.C.; Balkenhol, N.; Cushman, S.; Pérez, T.; Domínguez, A.; Saura, S. Estimating effective landscape distances and movement corridors: Comparison of habitat and genetic data. *Ecosphere* **2015**, *6*, art59. [[CrossRef](#)]
51. Xie, P.; Yang, J.; Wang, H.; Liu, Y.; Liu, Y. A New method of simulating urban ventilation corridors using circuit theory. *Sustain. Cities Soc.* **2020**, *59*, 102162. [[CrossRef](#)]
52. Lalechère, E.; Bergès, L. A Validation Procedure for ecological corridor Locations. *Land* **2021**, *10*, 1320. [[CrossRef](#)]
53. Kamwi, J.M.; Cho, M.A.; Kaetsch, C.; Manda, S.O.; Graz, F.P.; Chirwa, P.W. Assessing the spatial drivers of land use and land cover change in the protected and communal areas of the Zambezi Region, Namibia. *Land* **2018**, *7*, 131. [[CrossRef](#)]
54. Brennan, A.; Beytell, P.; Aschenborn, O.; Du Preez, P.; Funston, P.J.; Hanssen, L.; Kilian, J.W.; Stuart-Hill, G.; Taylor, R.D.; Naidoo, R. Characterizing multispecies connectivity across a transfrontier conservation landscape. *J. Appl. Ecol.* **2020**, *57*, 1700–1710. [[CrossRef](#)]
55. Kamusoko, C. Importance of remote sensing and land change modeling for urbanization studies. In *Urban Development in Asia and Africa*; Springer: Berlin/Heidelberg, Germany, 2017; pp. 3–10.
56. Kafy, A.-A.; Naim, N.H.; Khan, M.H.H.; Islam, M.A.; Al Rakib, A.; Al-Faisal, A.; Sarker, M.H.S. Prediction of urban expansion and identifying its impacts on the degradation of agricultural land: A machine learning-based remote-sensing approach in Rajshahi, Bangladesh. In *Re-Envisioning Remote Sensing Applications*; CRC Press: Boca Raton, FL, USA, 2021; pp. 85–106.
57. Jellason, N.P.; Robinson, E.J.; Chapman, A.S.; Neina, D.; Devenish, A.J.; Po, J.Y.; Adolph, B. A systematic review of drivers and constraints on agricultural expansion in sub-Saharan Africa. *Land* **2021**, *10*, 332. [[CrossRef](#)]
58. Baqa, M.F.; Chen, F.; Lu, L.; Qureshi, S.; Tariq, A.; Wang, S.; Jing, L.; Hamza, S.; Li, Q. Monitoring and Modeling the Patterns and Trends of Urban Growth Using Urban Sprawl Matrix and CA-Markov Model: A Case Study of Karachi, Pakistan. *Land* **2021**, *10*, 700. [[CrossRef](#)]
59. Ustaoglu, E.; Sisman, S.; Aydinoglu, A.C. Determining agricultural suitable land in peri-urban geography using GIS and Multi Criteria Decision Analysis (MCDA) techniques. *Ecol. Model.* **2021**, *455*, 109610. [[CrossRef](#)]
60. Woldesemayat, E.M.; Genovese, P.V. Monitoring urban expansion and urban green spaces change in addis ababa: Directional and zonal analysis integrated with landscape expansion index. *Forests* **2021**, *12*, 389. [[CrossRef](#)]
61. Terfa, B.K.; Chen, N.; Liu, D.; Zhang, X.; Niyogi, D. Urban expansion in Ethiopia from 1987 to 2017: Characteristics, spatial patterns, and driving forces. *Sustainability* **2019**, *11*, 2973. [[CrossRef](#)]

62. Monna, S.C. International Co-operation for the Management of the Okavango Basin and Delta. *Integr. Wetl. Water Resour. Manag.* **2000**, *4*, 107–112.
63. Abebe, M.T.; Megento, T.L. The City of Addis Ababa from 'Forest City' to 'Urban Heat Island' Assessment of Urban Green Space Dynamics. *J. Urban Environ. Eng.* **2016**, *10*, 254–262. [[CrossRef](#)]
64. Teferi, E.; Abraha, H. Urban heat island effect of Addis Ababa City: Implications of urban green spaces for climate change adaptation. In *Climate Change Adaptation in Africa*; Springer: Berlin/Heidelberg, Germany, 2017; pp. 539–552.
65. Zewdie, M.; Worku, H.; Bantider, A. Temporal dynamics of the driving factors of urban landscape change of addis ababa during the past three decades. *Environ. Manag.* **2018**, *61*, 132–146. [[CrossRef](#)]
66. Habibi, S.; Asadi, N. Causes, results and methods of controlling urban sprawl. *Procedia Eng.* **2011**, *21*, 133–141. [[CrossRef](#)]
67. Byrne, J.; Sipe, N. *Green and Open Space Planning for Urban Consolidation—A Review of the Literature and Best Practice*; Griffith University: Brisbane, QLD, Australia, 2010.
68. BenDor, T.K.; Metcalf, S.S.; Paich, M. The dynamics of brownfield redevelopment. *Sustainability* **2011**, *3*, 914–936. [[CrossRef](#)]
69. Andersson, J. *Land Cover Change in the Okavango River Basin: Historical Changes during the Angolan Civil War, Contributing Causes and Effects on Water Quality*; Tema Vatten i Natur Och Samhälle: Linköping, Sweden, 2006; Available online: <http://urn.kb.se/resolve?urn=urn:nbn:se:liu:diva-7152> (accessed on 17 July 2022).
70. Reliefweb. Angola Has 1220 Land Mine-Affected Areas. 28 September 2019. Available online: <https://reliefweb.int/report/angola/angola-has-1220-land-mine-affected-areas> (accessed on 7 February 2022).
71. Finckh, M.; Pröpper, M.; Autlwtse, B.; Roa, C.; De Cauwer, V.; Domptail, S.; Erb, C.; Espach, C.; Falk, T.; Fynn, R.; et al. The current status of the Okavango Basin. In *The Future Okavango—Findings, Scenarios and Recommendations for Action. Research Project Final Synthesis Report 2010–2015*; University of Hamburg: Hamburg, Germany, 2015; pp. 25–51.
72. Deininger, K.; Byerlee, D. *Rising Global Interest in Farmland: Can It Yield Sustainable and Equitable Benefits?* World Bank Publications: Washington, DC, USA, 2011.
73. Qiao, R.; Li, Y.; Cai, Y. Prediction of the Cultivated Land Demand Based on Logistic Equation—A Case of Zhejiang Province, China. *Asian Agric. Res.* **2009**, *1*, 49–52.
74. Kgathi, D.L.; Kniveton, D.; Ringrose, S.; Turton, A.R.; Vanderpost, C.H.; Lundqvist, J.; Seely, M. The Okavango; a river supporting its people, environment and economic development. *J. Hydrol.* **2006**, *331*, 3–17. [[CrossRef](#)]
75. Baumann, M.; Kuemmerle, T.; Elbakidze, M.; Ozdogan, M.; Radeloff, V.C.; Keuler, N.S.; Prishchepov, A.V.; Kruhlov, I.; Hostert, P. Patterns and drivers of post-socialist farmland abandonment in Western Ukraine. *Land Use Policy* **2011**, *28*, 552–562. [[CrossRef](#)]
76. Woods, K.; Elliott, S. Direct seeding for forest restoration on abandoned agricultural land in northern Thailand. *J. Trop. For. Sci.* **2004**, *16*, 248–259.
77. Magole, K.; Thapelo, L. The impact of extreme flooding of the okavango river on the livelihood of the molapo farming community of Tubu village, Ngamiland Sub-district, Botswana. *Botsw. Notes Rec.* **2005**, *37*, 125–137.
78. Bangira, T. *Mapping Surface Water in Complex and Heterogeneous Environments Using Remote Sensing*; Stellenbosch University: Stellenbosch, South Africa, 2019.
79. Brummett, R.E.; Lazard, J.; Moehl, J. African aquaculture: Realizing the potential. *Food Policy* **2008**, *33*, 371–385. [[CrossRef](#)]
80. Foucat, V.A. Community-based ecotourism management moving towards sustainability, in Ventanilla, Oaxaca, Mexico. *Ocean Coast. Manag.* **2002**, *45*, 511–529. [[CrossRef](#)]
81. Heinl, M. *Fire regime and Vegetation Response in the Okavango Delta, Botswana*; Technische Universität München: Munich, Germany, 2005.
82. Forno, I.W.; Smith, P.A. Management of the Alien Weed, *Salvinia molesta*, in the wetlands of the Okavango, Botswana. In *An International Perspective on Wetland Rehabilitation*; Streever, W., Ed.; Springer: Dordrecht, The Netherlands, 1999; pp. 159–166.
83. Ringrose, S.; Jellema, A.; Huntsman-Mapila, P.; Baker, L.; Brubaker, K. Use of remotely sensed data in the analysis of soil-vegetation changes along a drying gradient peripheral to the Okavango Delta, Botswana. *Int. J. Remote Sens.* **2005**, *26*, 4293–4319. [[CrossRef](#)]
84. Mogotsi, K.; Nyangito, M.M.; Nyariki, D.M. The role of drought among agro-pastoral communities in a semi-arid environment: The case of Botswana. *J. Arid Environ.* **2013**, *91*, 38–44. [[CrossRef](#)]
85. Gumbrecht, T.; McCarthy, T.S.; McCarthy, J.; Roy, D.; Frost, P.E.; Wessels, K. Remote sensing to detect sub-surface peat fires and peat fire scars in the Okavango Delta, Botswana. *S. Afr. J. Sci.* **2002**, *98*, 351–358.
86. Teshirogi, K.; Kanno, M.; Shinjo, H.; Uchida, S.; Tanaka, U. Distribution and dynamics of the *Cynodon dactylon* invasion to the cultivated fields of pearl millet in north-central Namibia. *J. Arid Environ.* **2022**, *205*, 104820. [[CrossRef](#)]
87. Kingston, D.G.; Mager, S.M.; Loft, J.; Underwood, G. An upstream–downstream/observation–model approach to quantify the human influence on drought. *Hydrol. Sci. J.* **2021**, *66*, 226–238. [[CrossRef](#)]
88. Ramberg, L.; Hancock, P.; Lindholm, M.; Meyer, T.; Ringrose, S.; Sliva, J.; Van As, J.; Vander Post, C. Species diversity of the Okavango delta, Botswana. *Aquat. Sci.* **2006**, *68*, 310–337. [[CrossRef](#)]
89. Gupta, R.; Sharma, L.K. Efficacy of Spatial Land Change Modeler as a forecasting indicator for anthropogenic change dynamics over five decades: A case study of Shoolpaneshwar Wildlife Sanctuary, Gujarat, India. *Ecol. Indic.* **2020**, *112*, 106171. [[CrossRef](#)]
90. Thonfeld, F.; Steinbach, S.; Muro, J.; Hentze, K.; Games, I.; Näschen, K.; Kauzeni, P.F. The impact of anthropogenic land use change on the protected areas of the Kilombero catchment, Tanzania. *ISPRS J. Photogramm. Remote Sens.* **2020**, *168*, 41–55. [[CrossRef](#)]

91. Tian, Y.; Yin, K.; Lu, D.; Hua, L.; Zhao, Q.; Wen, M. Examining Land Use and Land Cover Spatiotemporal Change and Driving Forces in Beijing from 1978 to 2010. *Remote Sens.* **2014**, *6*, 10593–10611. [[CrossRef](#)]
92. Sala, O.E.; Chapin, F.S.; Armesto, J.J.; Berlow, E.; Bloomfield, J.; Dirzo, R.; Huber-Sanwald, E.; Huenneke, L.F.; Jackson, R.B.; Kinzig, A. Global biodiversity scenarios for the year 2100. *Science* **2000**, *287*, 1770–1774. [[CrossRef](#)]
93. Shiferaw, H.; Alamirew, T.; Kassawmar, T.; Zeleke, G. Evaluating ecosystems services values due to land use transformation in the Gojeb watershed, Southwest Ethiopia. *Environ. Syst. Res.* **2021**, *10*, 22. [[CrossRef](#)]
94. Yuan, Z.; Xu, J.; Wang, Y.; Yan, B. Analyzing the influence of land use/land cover change on landscape pattern and ecosystem services in the Poyang Lake Region, China. *Environ. Sci. Pollut. Res.* **2021**, *28*, 27193–27206. [[CrossRef](#)]